PCCP

Accepted Manuscript

ROYAL SOCIETY OF CHEMISTRY

www.rsc.org/pccp

DOI: 10.1002/cphc.200((will be filled in by the editorial staff))

A 5-(difluorenyl)-1,10-phenanthroline-based Ru(II) complex as coating agent for potential multifunctional gold nanoparticles.

Juliette Moreau,[a] François Lux,[b] Mickaël Four,[a] Joanna Olesiak-Banska,[c] Katarzyna Matczyszyn,[c] Pascal Perriat,[d] Céline Frochot,[e,f] Philippe Arnoux,[d] Olivier Tillement,[b] Marek Samoc,[c] Glauco Ponterini,[g] Stéphane Roux,[h] and Gilles Lemercier*[a,f]

((Dedication, optional))

The synthesis and photophysical properties of small gold nanoparticles (NPs, ***AuNP-[Ru-PFF]****) surface functionalized by 5-substituted-1,10-phenanthroline-ligand based Ru(II) complexes are described. Luminescence of the grafted and confined Ru(II) complexes is totally quenched on the gold surface. Nonlinear optical properties were determined via Z-scan measurements in the range 600-1300 nm for both the free Ru(II) complex and the related NPs. In the short wavelength range (around 600 nm) the behaviour switches from that of two-photon absorption (2PA) for the complex to saturable absorption for the NPs. 2PA applications such as optical power limiting or two-photon dioxygen sensitization can be anticipated for these nanoplatforms*

Introduction

The development of functional multimodal nanostructures for applications[1] in catalysis,[2] sensing,[3] and medicine[4] (such as drug delivery,[5] cancer cell diagnostics,[6] and therapeutics[7]) are important directions that nanotechnology is presently taking. In this area, the design, synthesis, and characterizations of gold nanoparticles (Au-NPs) or nanorods (Au-NRs), have been at the forefront of these efforts[8] because of their their quite easy functionalization, their large variety of size and shape, their chemical stability, their biocompatibility[9] and their tunable optical properties (linear, but also third-order nonlinear optical properties such as saturable absorption[10] and two-photon excited luminescence,[11] for imaging and/or photodynamic therapy[12]). Multifunctional and multimodal nanoparticles (NPs)[13] are of particular interest in this domain, because they can exhibit enhanced efficiency and versatility by performing several tasks in parallel. For example, gadolinium(III) and radioisotope chelates coated gold nanoparticles, have been reported as contrast agents for both X-ray tomography and magnetic resonance imaging (MRI) and as radiotracers for medical nuclear imaging.[14] There are numerous studies in this field of research, following the method proposed by Brust *et al.*[15] Stable colloidal solutions of functionalized NPs can be generated in biphasic media and in the presence of a phase transfer agent (such as tetraoctylammonium, TOAB), by (*i*) direct functionalization with the pertinent agent also playing the role of stabilizing unit,[16] (*ii*) post-functionalization; the initial stabilizing ligand, being easily replaceable by the appropriate functionalizing agent.[17] Functionalization with inorganic compounds has emerged more recently.[18] It usually involves long alkyl thiol chains between the metallic surface and the coordination complexes,[19] but this interaction can also be ensured by one or two nitrogen atom(s).[20, 18b]

In parallel, Ru(II)-polypyridyl complexes have been intensively studied for their stability, inertness, and optical

---

[a] Dr. J. Moreau, Dr. M. Four, Pr. G. Lemercier
Institut de Chimie Moléculaire de Reims - UMR CNRS n° 7312
Reims Champagne-Ardenne University
Moulin de la Housse – BP 1039
51687 Reims Cedex 2 – France.
Fax: 0(+33)326913243
E-mail: gilles.lemercier@univ-reims.fr
[b] Dr. F. Lux, Pr. O. Tillement
Institut Lumière-Matière – Université de Lyon, Équipe Fennec
UMR CNRS n° 5306
69622 Villeurbanne, France.
[c] Dr. J. Olesiak-Banska, Dr. K. Matczyszyn, Pr. M. Samoc,
Institute of Physical and Theoretical Chemistry,
Wroclaw University of Technology,
Wybrzeze Wyspianskiego 27,
50-370 Wroclaw, Poland.
[d] Pr. P. Perriat,
Matériaux Ingénierie et Science, INSA-Lyon,
UMR 5510 CNRS, Université de Lyon,
69621 Villeurbanne Cedex, France.
[e] Dr. C. Frochot, P. Arnoux
Laboratoire Réactions et Génie des Procédés (LRGP), UMR CNRS n°7274, CNRS, Nancy, France
[f] GDR CNRS n° 3049 ''Médicaments Photoactivables - Photochimiothérapie (PHOTOMED)'', France
[g] Pr. G. Ponterini
Department of Life Sciences,
University of Modena and Reggio Emilia, via Campi 183,
41125 Modena, Italy.
[h] Pr. S. Roux,
Institut UTINAM - UMR 6213 CNRS-Université de Franche-Comté
Équipe Nanoparticules, Contaminants et Membranes,
25030 Besançon Cedex, France.

*Supporting information for this article is available on the WWW under http://www.chemphyschem.org or from the author.((****Please delete if not appropriate****))* properties such as second-order nonlinear optical properties,[21] two-photon absorption (2PA),[22] and triplet metal-to-ligand charge-transfer (^{3}MLCT) excited-state properties.[23] For example, one can take advantage of (*i*) the excited-state absorption for optical power limiting (OPL)[24] application, but also (*ii*) of the triplet character of the excited-state in order to use Ru(II) complexes as oxygen sensors[25] or sensitizers.[26] Recently, we reported the design of novel bifluorene-substituted 1,10-phenanthroline Ru(II) complexes for application in two-photon based OPL in the near-IR range. Optical power limiting aims at protecting detectors as well as the eyes from high-power pulsed lasers, and may result from a [2+1] photon process during the pulse (2PA and absorption of a third photon by the excited state). Although excited-state absorption (ESA) could be observed from singlet states of organic molecules, excited states with longer lifetimes, characteristic of metallic complexes such as Ru(II) compounds,[27] favour this phenomenon This held true, in particular, for Ru(II) compounds, thanks to their long-lived (around a microsecond) triplet metal-to-ligand excited state (^{3}MLCT).[23,28] The 2PA and ESA properties of these compounds were found to be strongly dependent on the π-conjugated ligands,[29] whether they bore one or two fluorene moieties as two-photon absorbers. For the present work, we have chosen Ru(II)-bifluorene units to functionalize small gold nanoparticles. Recently, gold nanoparticles-Ru(II) tris(2,2'-bipyridine) self assembled multi-structures have been reported to lead to a photocurrent response.[30] Mayer *et al*. showed that polypyridyl ruthenium complexes could be used as effective phase transfer agents.[31] Gunnlaugsson *et al*. described the first Ru(II) polypyridyl functionalized gold nanoparticles employed for applications as cellular imaging agents.[32]

In this study, we report on the synthesis, and the optical and photophysical properties of gold nanoparticles coated with new 1,10-phenanthroline-based Ru(II) complexes (**AuNP-[Ru-PFF]**) that make them good candidates as chromophores for 2PA-based optical power limiting (OPL), as a new oxygen sensor molecular material, or as two-photon sensitizers in photodynamic therapy (2PA-PDT). The synthesis of the Ru(II) complex which possesses a terminal alkyl disulfide group is described herein (see Scheme 1), while those of ligands **PFF**[33] and **LT-diS**[34] have already been published by some of us.

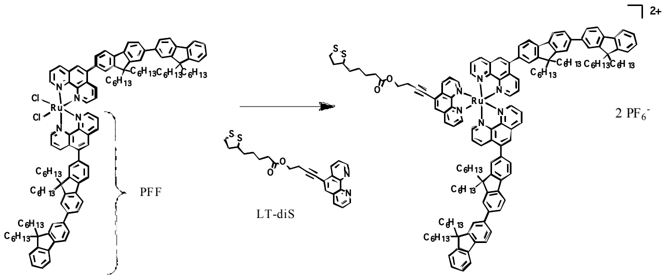

Scheme 1. Synthesis and molecular structure of **[Ru(PFF)$_2$LT-diS](PF$_6$)$_2$**

The synthesis of the related **AuNP-[Ru-PFF]** nanoparticles was achieved using the Brust method[15] based on the reduction of a gold salt (HAuCl$_4$, 3H$_2$O) by sodium borohydride (NaBH$_4$) in a biphasic water-toluene solution. The tetrachloroaurate anions were transferred by tetraoctylammonium ions from the aqueous solution to the organic phase which contains the ruthenium(II) complexes. This phase transfer was accompanied by the disappearance of the yellow colour of the aqueous phase. In order to ensure a precise control of the gold core and a high colloidal stability, the ruthenium(II) complexes were derivatized by a spacer arm ended with endocyclic disulphide bond since it was demonstrated that the presence of at least two sulphur atoms per ligand ensures a strong and long-standing adsorption of the stabilizing organic layer.[35]

Results and Discussion

Size and size distribution of the metallic nanoparticles. Size and size distribution were measured by means of dynamic light scattering (DLS). Figure 1 illustrates the typical size distribution of the Ru(II)-complex functionalized gold nanoparticles. The average size values correspond to a hydrodynamic diameter of 8.6 ± 0.3 nm at 20°C with a narrow size distribution, as polydispersity index values are low and show little variability between the different batches of particles prepared.

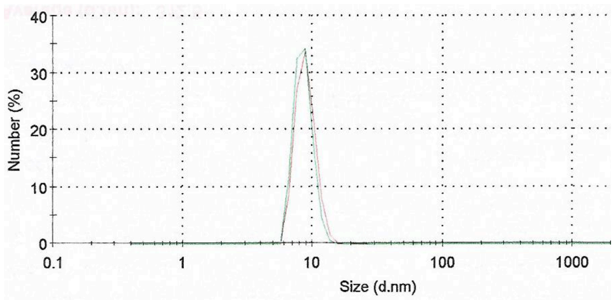

Figure 1. Typical size characterization of the gold nanoparticles using DLS distribution as a function of number %.

Microscopic characterizations Transmission electron microscopy (TEM) images of the gold nanoparticles are shown in Figure 2. Consistent with the DLS findings, the images obtained by TEM reveal that most of the nanoparticles are dispersed as individual NPs with a well-defined spherical shape and a low polydispersity with an average diameter of the metallic moiety around 2-3 nm when they are dehydrated. The difference in size is consistent with the existence of one layer of complexes grafted at the surface of the Au NPs (see Figure S1 in ESI).

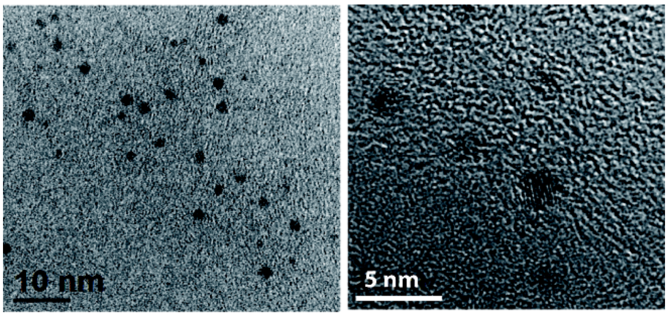

Figure 2. Transmission electron microscopy image of the Ru(II) complex-functionalized gold NPs

One-photon absorption and photophysics. The absorption spectrum of the complex **[Ru(PFF)$_2$LT-diS](PF$_6$)$_2$** is composed of (a) a broad band around 450 nm which corresponds to d(Ru^{II})→π^*-metal-to-ligand charge-transfer (^{1}MLCT) transitions and which is characteristic of this kind of ruthenium(II) complexes involving polypyridyl type ligands,[36] and (b) a broad and very intense band between 300 and 400 nm ($\lambda_{\max}$ around 330 nm in toluene), which, according to our previous work,[36] is due to an intra-ligand charge-transfer (ILCT) transition involving a charge flow from the fluorene units to the 1,10-phenanthroline moiety of the ligand. As shown in Figure 3, this band is observed at nearly the same wavelengths as for the free **PFF** ligand (λ_{max} = 340 nm). In both cases, the large width of this absorption band can be mainly ascribed to vibronic broadenings and/or the overlap of more bands corresponding to different close-lying electronic transitions. An analogous absorption spectrum is recorded for the related nano-suspension. However, an additional absorption band was observed around 510-530 nm, partially overlapping the MLCT absorption band of the Ru(II) complex. This is consistent with localised surface plasmon resonance (LSPR) of small gold nanoparticles.[37]

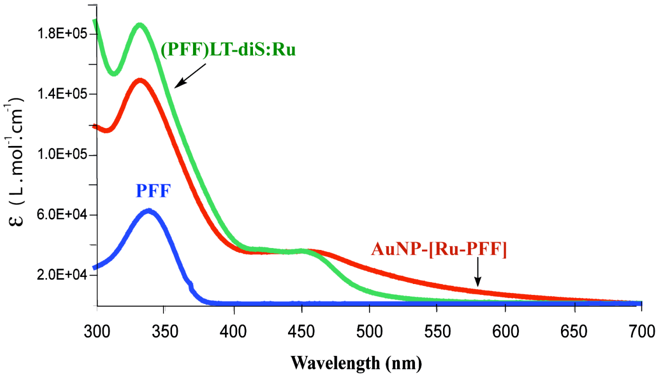

Figure 3. Absorption in toluene of the **PFF** ligand, **(PFF)LT-diS:Ru** complex (concentration of 5.8 10^{-6} and 3.3 10^{-6} mol.L^{-1}, respectively) and the related gold NPs (spectrum normalized to the absorbance at 450 nm).

Excitation into the MLCT band of **[Ru(PFF)$_2$LT-diS](PF$_6$)$_2$**, gives rise to an MLCT centred emission with maximum at 620 nm for the free complex. The corresponding excitation spectrum matches quite closely the absorption spectrum, apart from a pronounced shoulder around 360 nm. Solutions of the complex **[Ru(PFF)$_2$LT-diS](PF$_6$)$_2$** with Au NPs exhibit much weaker luminescence. The emission spectrum is similar to that of the Ru compound, *i.e.* a very similar shape and maximum, but with an additional broad emission at longer wavelengths (Figure 4). The excitation spectrum measured at an emission wavelength of 610 nm retains the shape of the absorption and related excitation spectra of the Ru compound; no contribution from the broad NPs absorption tail was observed, an indication of the absence of complex sensitization from plasmonic Au states.

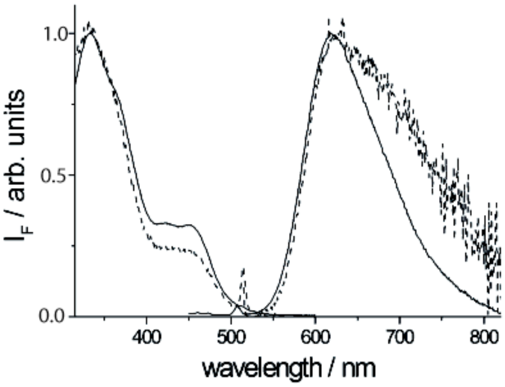

Figure 4. Excitation and emission spectra of **(PFF)LT-diS:Ru** (solid line) and its complex with Au Nps (dashed). λ_{exc} = 440 nm; λ_{em} = 610 nm. The spectra are normalized at their maxima for ease of comparison.

The emission quantum yield of the ruthenium complex and the apparent quantum yield of the related coated nanoparticles (see the experimental section) were 0.03 and 0.001 in CH_2Cl_2, respectively (see Table 1). This reveals a pronounced decrease in the emissive properties of the complex after chemical adsorption to the Au-NPs surface.

Table 1. Photophysical properties

	λ_{abs} (ε_{max})[a]	Attribution	λ_{em}[b]	λ_{exc}[c]	ϕL[d]	τ[e]
PFF[33]	272 (30500)	π-π* phen	427	278	0.900	ND
	365 (68300)	CT		375		
[Ru(PFF)$_2$LT-diS](PF$_6$)$_2$	271 (110100)	IL phen	619	333 366*sh*	0.030	200 (*aer*),
	333 (164900)	ILCT, MLCT		410-458		900 (deaer)
	410-460 (*plateau*)	MLCT				
AuNP-[Ru-PFF]	271 (110100)	IL phen	619	333 366*sh*	0.001	200 (*aer*),
	333 (164900)	ILCT, MLCT		410-458		900 (*deaer*)
	410-460 (*plateau*)	MLCT				

[a] Maximum linear absorption wavelength in nm (molecular absorption coefficients at λ_{max} in L mol^{-1} cm^{-1}) in chloroform; [b] Maximum emission wavelength in nm in dichloromethane; [c] λ_{exc} Maximum of the excitation spectra in nm; [d] ϕ_L luminescence quantum yield (%) in CH_2Cl_2 using *p*-bis(o-methylstyryl)benzene as reference (MSB. ϕ_L^{ref} = 1)[39] and in deoxygenated CH_2Cl_2 using $Ru(bipy)_3^{2+}$ (ϕ^{ref} = 0.062)[38] as reference for ligands and Ru(II) complexes, respectively;. [e] τ luminescence lifetimes in ns, in aerated and Ar purged toluene; ND: not determined; aer and deaer for aerated and deaerated solution, respectively.

The emissions at 610 nm of both **[Ru(PFF)$_2$LT-diS](PF$_6$)$_2$** and the corresponding coated Au NPs (in toluene) decayed mono-exponentially; the same lifetimes were obtained for the Ru compound and the coated NPs: 200 (±30) ns for air-equilibrated solutions and 900 (±80) ns for Ar-purged solutions. With an oxygen concentration around 2 x 10^{-3} mol L^{-1} for air-equilibrated toluene, we estimate a bimolecular quenching constant of about 2 x 10^{9} mol^{-1} L s^{-1}. This is about one fifth of the diffusion-controlled rate constant in toluene at 20 °C (k_{dif} = 1.1 x 10^{10} mol^{-1} L s^{-1})[38], *i.e.*, a value much lower than those typical for oxygen quenching of singlet-state solutes, for which all channels are spin-allowed and the total quenching rate constant is near k_{dif}.[40] However, it is also far from both the 1/9 k_{dif} and the 1/3 k_{dif} values characteristic of oxygen quenching of solutes in triplet states.[40]

The likeness of the emission lifetimes of the Ru(II) compound and its complexes with the Au NPs in toluene is hardly consistent with the strong emission quenching observed in steady-state experiments on the latter. Furthermore, apart from the apparent quantum yield, all the luminescence properties were the same for the two systems, including the excitation spectra that never included contributions from the absorption region of the Au NPs above 500 nm. For these reasons, we performed experiments to assess whether the very weak luminescence observed from solutions of the coated nanoparticles could be attributed to free emitting Ru complex in equilibrium with non-emitting Au-bound complex. In order to exploit the mass-action law, we measured steady-state emission intensities of air-equilibrated toluene solutions of the two species at different solute concentrations. The latter were monitored spectrophotometrically and characterized in terms of A_{420}, the absorbance at 420 nm, the excitation wavelength employed in these experiments. For each value of A_{420}, the emission intensities at 610 nm were corrected for the slightly different absorbance in order to obtain a relative apparent emission quantum yield, R. The results in Figure 5, clearly indicate that this property strongly depends on the sample concentration, even after correction for the inner-filter effect at 610 nm (see the details in the Experimental section).

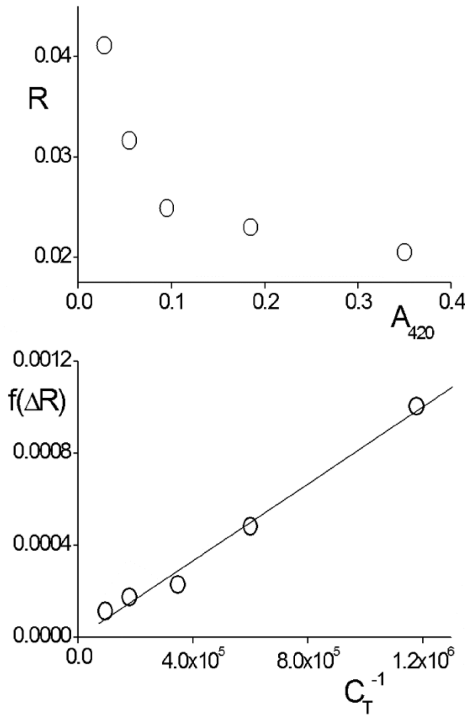

Figure 5. Top: relative emission quantum yields (R) of the coated Au NPs *vs.* the Ru complex as functions of the Ru-complex concentration. (A_{420} = absorbance at 420 nm, the excitation wavelength). Bottom: equilibrium analysis of Ru-complex/Au Nps binding according to eq. 1 (see the text and the Supplementary Information). f(*Δ*R) is the left member in eq. 1; C_T = total molar concentration of the Ru complex.

This indicates an increase in the equilibrium fraction of free, emitting Ru(II) compounds with decreasing concentration of its complexes with the Au NPs. To prove that the reported dependence does not arise from experimental artefacts, the intensities of **[Ru(PFF)$_2$LT-diS](PF$_6$)$_2$** emission at 610 nm as a function of its absorbance at 420 nm is reported in Figure S2 (see the Supplementary Information). The emission intensity scales linearly with the absorbance almost up to an A_{420} of 0.3, and a loss of linearity could only slightly affect the result corresponding to the highest concentration. Based on this reported evidence, binding to the Au NPs causes a quenching of the free Ru(II) complex emission more pronounced than reported in Table 1. A *ratio* of 60 between the **[Ru(PFF)$_2$LT-diS](PF$_6$)$_2$** and the related coated NPs emission yields, corresponding to the largest concentration in Figure 5, is likely a lower limit for this residual *ratio*.

Binding equilibrium Results in Figure 6 can also be employed to quantitatively characterize the equilibrium between the Au NPs/Ru-compound complexes (SC) and free Ru-complexes (C), and Au NPs binding sites (S): $SC \rightleftharpoons S + C$. This analysis is reported in the Supplementary Information and yields equation 1

$$\frac{\Delta R^2}{(1-\Delta R)} = \frac{K_D}{C_T} \quad \text{eq. 1}$$

where K_D is the dissociation equilibrium constant, R the ratio of the emission intensities of a solution of coated Au NPs and a solution of the Ru complex having the same Ru complex concentration, C_T, and $\Delta R = R - R^{\infty}$, where R^{∞} is the limit value of R at high C_Ts, *i.e.*, at negligibly small fraction of dissociated SC complexes. We obtain a good fitting (lower panel in Figure 5 with R^{∞} = 0.01, and, from the slope, estimate K_D = 8 x 10^{-10} mol l^{-1}, corresponding to $\Delta G°$= 39.8 kJ mol^{-1}. The R limiting value implies the luminescence emission of the Ru-complex to be reduced by two orders of magnitude upon binding to the Au NPs; thus the latter act as efficient excitation energy sinks.

Energy transfer between the ^{3}MLCT state and the fundamental triplet state of dioxygen has been studied in order to evaluate the potential photosensitizer abilities (singlet oxygen $^1O_2$ formation) of the grafted ruthenium complexes. Oxygen is a dynamic or collisional quencher of the complexes. In fluid solution, the dependence of emission intensity and lifetime with quencher concentration is given by the Stern-Volmer equation (see text and Figures S3 in ESI); as shown in Figure S3, the slopes were determined and equal to 6.2. Exactly the same result was obtained with the gold NPs. It could be assumed that **[Ru(PFF)$_2$LT-diS](PF$_6$)$_2$** and the related nanoparticles react in the same manner with the dioxygen, and it could be in good agreement with the small size of these nano-objects and non-aggregated character of the NPs in the solution; nevertheless, it is more probably the confirmation of the non-luminescent character of the grafted Ru(II) complexes, the measured emission being due to the small amount of free **[Ru(PFF)$_2$LT-diS](PF$_6$)$_2$** complexes in solution. Nevertheless, direct determination of the formed $^1O_2$ amount was performed *via* luminescence measurement in toluene at 1270 nm (see Figure S4 in ESI). Excitation was performed at 420 nm, in the ^{3}MLCT absorption band, and out of the plasmon absorption spectral area. The quantum yield (ϕ_Δ) of $^1O_2$ production was deduced to be around 40-50% of the one of the Rose Bengal (taken as a reference) in the same conditions. The photosensitivity of the nanoparticles for dioxygen was quite high and cannot be attributed to the small amount of free complex in solution; this renders these objects and related suspensions, pertinent as oxygen sensitizer nano-platforms.

Nonlinear optical properties and Z-scan measurements. Two-photon spectra in the 550 to 1300 nm range were measured using the Z-scan technique. Taking into account the size of an NP (d = 2 nm), and assuming the density of the material equal to that of bulk gold (19.300 kg/m^3) we determined the mass of a single nanoparticle. Then, basing on the radius of NP, we calculated the average number of Ru molecules attached to one NP to be around 100 (see supplementary information for the calculation). Thus, the molar weight of a functionalized nanoparticle is around 320500 g/mol and molar absorption coefficients can therefore be deduced (see Figure S5 in ESI). The nonlinear refractive index of the functionalized nanoparticles was found to have negative values in the range 550 - 850 nm.

Figure 6 shows two-photon absorption spectra of AuRu and Ru samples presented together with the corresponding one-photon absorption spectra plotted at twice the wavelength. At λ = 675 nm, which corresponds to the two-photon absorption in the ILCT (intra-ligand charge-transfer) band the two-photon absorption cross-section (σ_2) of a free Ru(II) complex molecule in the solution is found to be appr. 3000 GM (GM stands for the Goeppert-Mayer unit = 10^{-50} cm^{4}s) while dividing the cross section of a decorated nanoparticle by the number of the ligands attached to it gives around 3200 GM. Thus practically no increase of the σ_2 value is observed. A lack of a significant plasmonic enhancement can be explained by the small size of nanoparticles, which, being close to 2-3 nm in diameter, are almost at the border below which gold nanostructures present discrete rather than band electronic structure and are treated as clusters. Even higher two-photon absorption is observed for the free complex molecule irradiated at 600 nm (IL 1,10-phenanthroline transition), with σ_2 = 7000 GM (see values in Table S1 in ESI). When the complex molecules are attached to nanoparticles, negative values of the two-photon absorption cross-section are calculated in this wavelength range, which originate from saturation of one-photon absorption present in that range of wavelengths. Therefore, the attachment of the [Ru] ligands to Au nanoparticles results in a switch from 2PA properties to saturable absorption. This phenomenon is akin to the reported in the literature electrochemical switching of the third-order nonlinearity.[41]

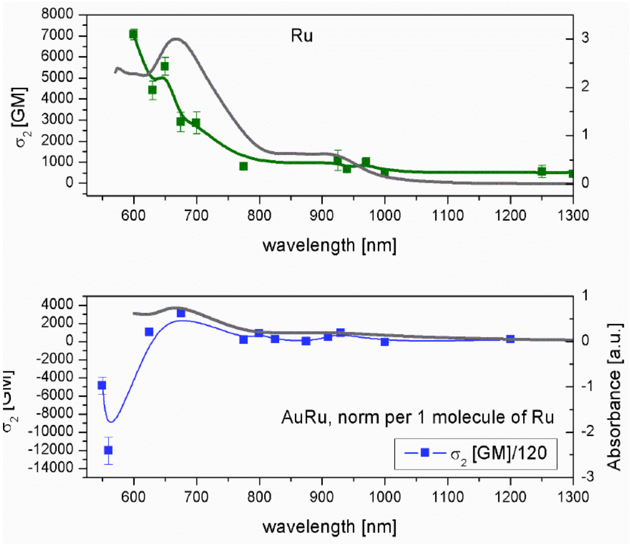

Figure 6. Two-photon absorption spectra (measured by Z-Scan) for free Ru complex (**[Ru(PFF)$_2$LT-diS](PF$_6$)$_2$**, top) and the related gold nanoparticles (down); one-photon absorption plotted at twice the wavelength is presented for comparison.

Figure 7 presents examples of Z-scan traces measured with closed-aperture (CA) and open-aperture (OA) configuration. Plots a and b represent examples of response of both Ru-based ligand and functionalized nanoparticles solutions.

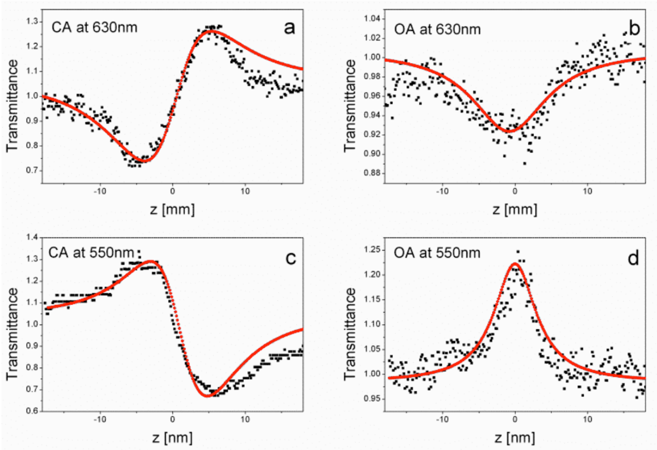

Figure 7. Examples of Z-scan traces (and related fitting curves) measured with closed-aperture (CA, a and c) and open-aperture (OA, b and d) configuration for both free Ru-based ligand and related gold NPs at 630 (a and b) and for functionalized NPs at 550 nm (c and d).

For the spectral range 550-600 nm, saturation of one-photon absorption was observed for the NPs (and not for the free Ru(II) complexes), which is a characteristic nonlinear response of plasmonic nanoparticles solution for illumination in the localised surface plasmon resonance band.[10]

Conclusion

In this study, we show that gold surface functionalization can be an efficient way to obtain the confinement of chromophores at the surface of new multifunctional nano-platforms. This can lead to obtaining modified linear and nonlinear photophysical properties that arise from the combination of the additivity of the cross sections of the components and the interplay of the properties of the chromophore and the metal nanoparticle. Z-Scan measurements reveal two-photon absorption properties for both free Ru(II) complexes and related NPs. Around 600 nm, 2PA properties are switched to saturable absorption for the NPs. In order to get more insight into this system, we intend to investigate the influence of the NPs size on its photophysical properties. Applications such as optical power limiting and oxygen sensitization can be anticipated. In this area, multifunctional nanoparticles are also of particular interest because they can exhibit enhanced efficiency and versatility by performing several tasks in parallel. To this aim, a gold–surface co-functionalization with rare-earth complexes is also in progress.[42]

Experimental Section

Synthesis

^{1}H and ^{13}C NMR spectra were recorded on a Bruker DPX 200 spectrometer (at 200.13 MHz for ^{1}H and 50.32 MHz for ^{13}C) and also on a Varian Unity Plus at 499.84 MHz for ^{1}H. Elemental analysis were carried out by the Service Central d'Analyse, CNRS. UV/Vis spectra were recorded in the 200-800 nm range on a UV/Vis Jasco V-550; λ_{max} are given in nm and molar extinction coefficients ε in L.mol^{-1}.cm^{-1}.

Synthesis and characterizations of ligands **PFF**[33] and **LT-diS**[34] have already been described.

Ru(PFF)$_2$Cl$_2$: 100 mg of $RuCl_3.3H_2O$ (0.39 mmol, 1 eq.) and 160 mg of LiCl (3.86 mmol, 10 eq.) were dissolved in DMF, under argon. A DMF solution of 659 mg of PFF (0.78 mmol, 2 eq.) was dropwise added, and the mixture was refluxed for 3.5 h. Saturated aqueous solution of NH_4PF_6 was then added to the resulting solution at room temperature. The precipitate was collected by filtration, washed three times with water and twice with pentane, dissolved in dichloromethane and dried over Na_2SO_4. After filtration and evaporation, the desired complex was purified by two recristallizations in a mixture pentane/dichloromethane. 505 mg of solid was obtained. Yield: 70%. IR (cm^{-1}) 3450 (water), 3057, 2927 (DMF), 2852 (DMF), 1974 (DMF), 1616, 1455, 1522, 1374, 888, 822, 738. Anal. Calcd for $RuC_{124}H_{144}N_4OCl_2$, 0.5 DMF, 1.5 H_2O: C, 78.26; H, 7.88; N, 3.27. Found: C, 78.40; H, 7.68; N, 3.05%.

[Ru(PFF)$_2$LT-diS](PF$_6$)$_2$ The ligand **LT-diS** (51 mg, 0.12 mmol) and complex Ru(PFF)$_2$Cl$_2$ (218 mg, 0.12 mmol) were dissolved, under argon, in 8 mL of DMF. The mixture was heating at reflux for a night. Saturated aqueous solution of NH_4PF_6 was then added to the resulting solution at room temperature. The precipitate was collected by filtration, washed two times with water and one time with hexane. 237 mg of a red powder was obtained. Yield: 72%. ^{1}H NMR (250.13 MHz, $CDCl_3$) δ (ppm): 8.9-8.7 (2H, m), 8.5 (4H, m), 8.1-8.0 (8H, m), 7.8-7.7 (30H, m), 7.3 (6H, m), 4.4 (2H, m), 3.5 (1H, m), 2.3-1.5 (29H, m), 1.0 (48H; m), 0.73 (40H, m). IR ν (cm^{-1}) 2927 (DMF), 2855 (DMF), 1978 (DMF), 1729, 1622, 844, 733, 558. Anal. Cacld for. $RuC_{148}H_{168}N_6O_2S_2P_2F_{12}$, 2 DMF, 3.5 H_2O: C, 67.82; H, 6.98; N, 4.11; Ru, 3.72. Found: C, 67.54; H, 6.73; N, 4.50; Ru, 4.34.

AuNP-[Ru-PFF] An aqueous solution of $HAuCl_4.3H_2O$ (31 mg, 0.079 mmol) in H_2O (6 mL) was mixed with an organic solution of tetraoctylammonium bromide (TOAB) (197 mg, 0.360 mmol) in toluene (16 mL); stirring was performed magnetically until the gold salt was transferred to the organic layer. 200 mg of C2 complex solubilised in 6 mL of toluene was added at the mixture (0.0733 mmol) and finally, a freshly prepared solution of $NaBH_4$ (33 mg) in water (5 mL) was added. The two-phases mixture was vigorously stirred using a magnetic stirrer for 3h, leading to a dark solution. After elimination of the aqueous layer, the organic phase was washed two times with water. 100 mL of EtOH was added and the mixture kept at -18°C overnight. The precipitate was collected by filtration (nylon membrane, pore 0.2 μm) and washed three times with EtOH. 36 mg of a black powder was obtained. IR (cm^{-1}) 3500 (water), 2954, 2926, 2854 (DMF), 1974 (DMF), 1670, 1560, 1450, 843, 741, 557, 484. Anal. Calcd. for Ru(PFF)$_2$LT-diS, 2PF$_6^-$, 2 Au, 1 DMF: C, 60.76; N, 3.28; Ru, 3.39; Au, 13.20. Found: C, 60.39; N, 3.32; Ru, 3.39; Au, 14.22%.

Physical measurements

Luminescence: Steady-state luminescence spectra were measured with a Spex-Jobin Yvon Fluoromax2 spectrofluorometer and were corrected for the instrumental spectral sensitivity. Luminescence lifetimes were measured for an air-equilibrated **(PFF)LT-diS:Ru** solution with an IBH-5000 time-correlated single-photon counting equipment using an excitation wavelength of 450 nm and an emission wavelength of 610 nm. The lifetimes of both compounds in air-equilibrated and Ar-purged toluene solutions were measured using the second harmonic of a Nd-YAG laser (532 nm, ca. 10 ns FWHM) as the excitation source, and a monochromator (set at 610 nm) with a photomultiplier (2 ns resolution) as the detection system. Measurements were performed at 18 °C on samples with absorbances at 532 nm around 0.03 and 0.3 for **(PFF)LT-diS:Ru** and coated Au Nps, respectively. For the air-equilibrated Ru-complex solution, the two measurement approaches gave consistent results.

Inner-filter effect due to the absorption of the Au nanoparticles at 610 nm in the concentration-dependent steady-state experiments (Figure GP2) were estimated and the **(PFF) LT-diS:Ru**/coated Au NPs relative emission yields were corrected for this effect by multiplying them by $10^{A610/2}$ [38]. Emission quantum yields ϕ_L were determined at 25°C in deoxygenated acetonitrile solutions using a CH_3CN solution of $[Ru(Phen)_3](PF_6^-)_2$ (ϕ_L^{ref}= 0.03)[43] molar solution in water as a standard, according to equation (1),

$$\varphi_L^S = \frac{I_L^S}{I_L^{\mathrm{Ref}}} \frac{(1-10^{-OD^{\mathrm{Ref}}})}{(1-10^{-OD^S})} \varphi_L^{\mathrm{Ref}} \qquad (1)$$

where I_L, the emission intensity, was calculated from the spectrum area $\int I(\lambda)d\lambda$, OD represents the optical density at the excitation wavelength. The superscripts "S" and "Ref" refer to the sample and the standard, respectively. n is the refractive index for each solvent. The luminescence lifetime of the complexes **C1** and **C2** were measured after irradiation at λ = 337 nm obtained with a 4 ns pulsed N_2 laser (Optilas VSL-337ND-S) and recorded at the emission maximum wavelength using a monochromator and a photomultiplier tube (Hamamatsu R928) coupled with an ultra-fast oscilloscope (Tektronix TDS 520A).

The Z–scan technique[44] was used to determine both the nonlinear refraction and nonlinear absorption of bulk samples. Solutions of the ligand and ligated nanoparticles in toluene were placed in a 1mm glass cell that was made to travel along the focused Gaussian-shaped laser beam.[45] Closed aperture (CA) and open aperture (OA) Z-scan traces were recorded simultaneously in a single Z-scan run and used to determine the bulk nonlinear optical parameters of the solutions. In principle, recording just OA traces would be sufficient for the measurements of nonlinear absorption, however our experimental routine calls for recording both OA and CA traces, the CA traces taken for a fused silica sample being used for the calibration of the light intensities. ~130 fs pulses were delivered by a laser system consisting of a Quantronix Integra-C regenerative amplifier operating as an 800 nm pump and a Quantronix-Palitra-FS BIBO crystal-based optical parametric amplifier, with the repetition rate of 1 kHz. The output from the Palitra was appropriately filtered using wavelength separators and color glass filters. It was then attenuated to microjoule per pulse energy range. The beam was focused to a focal spot with the beam waist w_0 = 25 – 60 μm, which resulted in peak intensities in the range from 60 to 150 GW cm^{-2}. Three InGaAs photodiodes (Thorlabs) collected the reference signal, the OA signal, and the CA signal. The data was analyzed as described[46] in order to obtain microscopic nonlinear optical parameters of the ligand molecules and ligated nanoparticles.

Dynamic light scattering (DLS) was used for the measurement of average hydrodynamic diameters and polydispersity indexes (PdI) (Malvern Zetasizer Nano-ZS, Malvern Instruments, UK). Each sample was analyzed in triplicate at 20°C at a scattering angle of 173°. Pure water was used as a reference dispersing medium.

Transmission electron microscopy (TEM). Images were acquired using a JEOL 2010 F microscope operating at 200 kV. Particles are observed after deposition of a drop of the gold colloidal solution on a copper grid coated by a thin film of carbon.

Acknowledgements

The authors thank G. Boeuf for the Stern-Volmer measurements and G. Roullin for the DLS results; GL thanks F. Paul, O. Mongin for help, and M. G. Humphrey for fruitful discussion.

Keywords: Functionalized *Au nanoparticles, Ru(II) complexes, ^{3}MLCT excited-state, two-photon absorption, Z-scan measurements.*

[1] H. Goesmann, C. Feldmann, *Angew. Chem.; Int. Ed.* **2010**, *49*, 1362-1395.

[2] A. T. Bell, *Science*, **2003**, *299*, 1688-1691.

[3] a) U. H. F. Bunz, V. M. Rotello, *Angew. Chem., Int. Ed.* **2010**, *49*, 3268-3279 ; b) A. Labande, J. Ruiz, D. Astruc, *J. Am. Chem. Soc.* **2002**, *124,* 1782-1789.

[4] Special issue *Acc. Chem. Res*. and references therein, **2011**, *44* ; b) C. Kim, S. S. Agasti, Z. Zhu, L. Isaacs, V. M. Rotello, *Nat Chem*. **2010**, 2, 962; N. L. Rosi, C. A. Mirkin, *Chem. Rev*. **2005**, 105, 1547.

[5] a) G. F. Paciotti, L. Myer, D. Weinreich, D. Goai, N. Pavel, R. E. Mclaughlin, L. Tamarkin, *Drug delivery* **2004**, 11, 169-183.

[6] a) X. Lu, H. Liu, J. Liu, K. N. Haley, J. A. Treadway, J. P. Larson, N. Ge, F. Peale, M. P. Bruchez, *Nat. Biotechnol*., **2003**, *21*, 41-46 ; b) A. P. Alivisatos, *Nat. Biotechnol*. **2004**, *22*, 47-52.

[7] a) L. R. Hirsch, R.J. Stafford, J. A. Bankson, S. R. Sershen, B. Rivera, R. E. Rrice, J. D. Hazle, N. J. Halas, J. L. West, *Proc Natl. Acad. Sci USA* **2003**, 100, 13549-13554 ; b) Y. Cheng, A. C. Samia, J. D. Myers, J. I. Panagopoulos, B. W. Fei, C. Burda, *J. Am. Chem. Soc.* **2008**, *130*, 10643-10647; c) S. D. Brown, P. Nativo, J. A. Smith, D. Stirling, P. R. Edwards, B. Venugopal, D. J. Flint, J. A. Plumb, D. Graham, N. J. Wheate, *J. Am. Chem. Soc.* **2010**, *132*, 4678-4684.

[8] M. Hu, J. Chen, Z.-Y. Li, L. Au, G. V. Hartland, X. Li, M. Marquez, Y. Xia, *Chem. Soc. Rev*. **2006**, *35*, 1084-1094 ; J. Cao, T. Sun, K. T. V. Grattan, *Sensors and Actuators B : Chem*. **2014**, *195*, 332-351.

[9] M. C. Daniel, D. Astruc, *Chem. Rev*. **2004**, *104*, 293-346 ; B. L. Cushing, V.L. Kolesnichenko, C.J. O'Connor, *Chem. Rev*. **2004**, *104*, 3893-3946.

[10] J. Olesiak-Banska, M. Gordel, R. Kolkowski, K. Matczyszyn, M. Samoc, *J. Phys. Chem. C* **2012**, *116*, 13731−13737.

[11] P. Genuche, S. Cherukulappurath, T. H. Taminiau, N. F. van Hulst, R. Quidant *Phys. Rev. Lett*., **2008**, *101*, 116805-1-4; L. Tong, Q. Wei, A. Wei, J.-X. Cheng *Photochem. and photobiol*, **2009**, *85*, 21-32; Z. Guan, N. Gao, X.-F. Jiang, P. Yuan, F. Han, Q.-H. Xu, *J. Am. Chem. Soc.* **2013**, *135*, 7272−7277.

[12] T. T. Zhao, X. Q. Shen, L. Li, Z. P. Guan, N. Y. Gao, P. Y. Yuan$_{\#}$S. Q. Yao, Q$_{\#}$. H. Xu, G. Q. Xu *Nanoscale* **2012**, *4*, 7712−7719 ; T. Zhao, X.-F. Jiang, N. Gao, S. Li, N. Zhou, R. Ma, Q.-H. Xu *J. Phys. Chem. B* **2013**, *117*, 15576−15583.

[13] a) Q. A. Pankhurst, J. Connolly, S. K. Jones, J. Dobson, *J. Phys. D-Appl. Phys.* **2003**, *36*, R167-R181. b) A. K. Gupta, M. Gupta, *Biomaterials* **2005**, *26*, 3995-4021. c) J. Yang, C. H. Lee, H. J. Ko, J. S. Suh, H. G. Yoon, K. Lee, Y. M. Huh, S. Haam, *Angew. Chem.-Int. Ed.* **2007**, *46*, 8836-8839. d) J. Gao, W. Zhang, P. Huang, B. Zhang, X. Zhang, B. J. Xu, *J. Am. Chem. Soc*. **2008**, *130*, 3710-3711; e) M. K. Yu, Y. Y. Jeong, J. Park, J. W. Kim, J. J. Min, K. Kim, S. Jon, *Angew. Chem., Int. Ed.* **2008**, *47*, 5362-5365; f) J. H. Lee, B. Schneider, E. K. Jardon, W. Liu, J. A. Frank, *Adv. Mater*., **2008**, *20*, 2512-2516 ; g) J. Olesiak-Banska, M. Gordel, K. Matczyszyn, V. Shynkar, J. Zyss, M. Samoc, *Nanoscale* **2013**, 5, 10975-10981.

[14] a) C. Alric, J. Taleb, G. Le Duc, C. Mandon, C. Billotey, A. Le Meur-Herland, T. Brochard, F. Vocanson, M. Janier, P. Perriat, S. Roux, O. Tillement, *J. Am. Chem. Soc.* **2008**, *130*, 5908-5913; b) D. R. Arifin, C. M. Long, A. A. Gilad, C. Alric, S. Roux, O. Tillement, T. W. Link, A. Arepally, J. W. M. Bulte, *Radiology*, **2011**, *260*, 790-798. c) C. Alric, I. Miladi, D. Krysa, J. Taleb, F. Lux, R. Bazzi, C. Billotey, M. Janier, P. Perriat, S. Roux, O. Tillement, *Nanoscale* **2013**, *5*, 5930-5939.

[15] a) M. Brust, M. Walker, D. Bethell, D.-J. Schiffrin, R.-J. Whyman, *J. Chem. Soc. Chem. Commun*. **1994**, 801-802 ; b) M. Brust, J. Fink, D. Bethell, D. J. Schiffrin, C. J. Kiely, *J. Chem. Soc., Chem. Commun*. **1995**, 1655-1656.

[16] C. R. Mayer, S. Neveu, V. Cabuil, *Angew. Chem. Int. Ed. Engl.* **2002**, *41*, 501-503.

[17] S.-Y. Lin, Y.-T. Tsai, C.-C. Chen, C.-M. Lin, C.-H. Chen, *J. Phys. Chem. B* **2004**, *108*, 2134-2139.

[18] a) J. Massue, S. J. Quinn, T. Gunnlaugsson, *J. Am. Chem. Soc.* **2008**, *130*, 6900-6901 ; b) C. R. Mayer, E. Dumas, F. Sécheresse, *Chem. Commun*., **2005**, 345-347.

[19] M. C. Daniel, J. Ruiz, S. Nlate, J.-C. Blais, D. Astruc, *J. Am. Chem. Soc.* **2003**, *125*, 2617-2628

[20] a) C. R. Mayer, G. Cucchiaro, J. Jullien, F. Dumur, J. Marrot, E. Dumas, F. Sécheresse, *Eur. J. Inorg. Chem*. **2008**, 3614-3623 ; b) C. R. Mayer, E. Dumas, A. Michel, F. Sécheresse, *Chem. Commun*. **2006**, *40*, 4183-4185.

[21] O. Maury, H. Le Bozec Acc. Chem. Res., **2005**, *38*, 691-704 ; L. Boubekeur-Lecaque, B. J. Coe, J. A. Harris, M. Helliwell, I. Asselberghs, K. Clays, S. Foerrier, T. Verbiest, *Inorg. Chem*. **2011**, *50*, 12886-12899 ; B. Coe, J. A. Harris, B. S. Brunschwig, I. Asselberghs, K. Clays, J. Garin, J. Orduna *J. Am. Chem. Soc*., **2005**, *127*, 13399-13410.

[22] M. Samoc, J. P. Morrall, G. T. Dalton, M. P. Cifuentes and M. G. Humphrey, *Angew. Chem. Int. Ed.* **2007**, *46*, 731-733 ; G. Lemercier, A. Bonne, M. Four, L. M. Lawson-Daku, *C. R. Chimie* **2008**, *11*, 709-715**.**

[23] A. Juris, V. Balzani, F. Barigelletti, S. Campagna, P. Belser and A.Von Zelewsky, *Coord. Chem. Rev*. 1988, **84**, 85-277.

[24] M. G. Humphrey, B. Lockhart-Gillet, M. Samoc, B. W. Skelton, V.-A. Tolhurst, A. H. White, A. J. Wilson and B. F. Yates, *J. Organomet. Chem.* **2005**, *690*, 1487-1497 ; C. E. Powell, M. P. Cifuentes, M. G. Humphrey, A.C. Willis, J. P. Morrall, M. Samoc, *Polyhedron* **2007**, *26*, 284-289 ; T. V. Duncan, P. R. Frail, I. R. Miloradovic and M. J. Therien, *J. Phys. Chem. B,* **2010**, *114*, 14696-14702.

[25] a) P. Hartmann, W. Ziegler, *Anal. Chem*. **1996**, *68*, 4512-4514 ; b) B. Elias, A. Kirsch-De Mesmaeker, *Coord. Chem. Rev*. **2006**, *250,* 1627-1641.

[26] Tan-Sien-Hee, L.; Jacquet, L.; Kirsch-De Mesmaeker, A., *J. Photochem. Photobiol. A : Chem*. **1994**, *81*, 169-176; (a) Abdel-Shafi, A. A.; Beer, P. D.; Mortimer, R. J.; Wilkinson, F., *PhysChemChemPhys* **2000**, *2*, 3137-3144; (b) Abdel-Shafi, A. A.; Beer, P. D.; Mortimer, R. J.; Wilkinson, F., *J. Phys. Chem. A*. **2000**, *104*, 192-202 ; (c) F. Schmitt, P. Govndaswamy, G.Süss-Fink, W. H.; Ang, P. J. Dyson, L. Juillerat-Jeanneret, B. Therrien, *J. Med. Chem*. **2008**, *51*, 1811-1816 ; (d) Y. Liu,; R. Hammitt, D. A. Lutterman, L. E. Joyce, R. P. Thummel, C. Turro, *Inorg. Chem*. **2009**, *48*, 375-385; (e) C. Boca, M. Four, A. Bonne, B. van Der Sanden, S. Astilean P. L. Baldeck, G. Lemercier, *Chem. Commun.* **2009**, 4590-4592.

[27] C. Girardot, B. Cao, J.-C. Mulatier, P. L. Baldeck, J. Chauvin, D. Riehl, J. A. Delaire, C. Andraud, G. Lemercier, *ChemPhysChem*. 2008, **9**, 1531-1535.

[28] V. Caspar, T. J. Meyer, *J. Am. Chem. Soc*. 1983, **105**, 5583-5590.

[29] M. Four, D. Riehl, O. Mongin, M. Blanchard-Desce, L. Max Lawson-Daku, J. Moreau, J. Chauvin, J. A. Delaire, G. Lemercier, *PhysChemChemPhys.* **2011**, *13*, 17304-17312.

[30] Y. Kuwahara, T. Akiyama, S. Yamada, *Thin Solid Films* **2001**, *393*, 273-277.

[31] C. R. Mayer, E. Dumas, F. Sécheresse, J. *Colloid and Interface Science* **2008**, *328*, 452-457 ; C. R. Mayer, E. Dumas, F. Miomandre, R. Méallet-Renault, F. Warmont, J. Vigneron, R. Pansu, A. Etcheberry, F. Sécheresse, *New J. Chem*. **2006**, *30*, 1628-1637.

[32] R. B. P. Elmes, K. N. Orange, S. M. Cloonan, D. C. Williams, T. Gunnlaugsson, *J. Am. Chem. Soc*. **2011**, *133*, 15862-15865.

[33] C. Girardot, G. Lemercier, J.-C. Mulatier, C. Andraud, J. Chauvin, P. L. Baldeck, *Tetrahedron Lett.,* **2008**, *49*, 1753-1758.

[34] F. Lux, F. Lerouge, J. Bosson, G. Lemercier, C. Andraud, G. Vitrant, P. L. Baldeck, F. Chassagneux, S. Parola, *Nanotechnology.* **2009**, *20*, 355603 (6pp).

[35] a) B. Garcia, M. Salomé, L. Lemelle, J.-L. Bridot, P. Gillet, P. Perriat, S. Roux, O. Tillement, *Chem. Commun.* **2005**, 369-371; b) S. Roux, B. Garcia, J.-L. Bridot, M. Salomé, C. Marquette, L. Lemelle, P. Gillet, L. Blum, P. Perriat, O. Tillement, *Langmuir* **2005**, *21*, 2526-2536; c) Z. Li, R. Jin, C. A. Mirkin, R. L. Letsinger, *Nucleic Acids Res.* **2002**, *30*, 1558-1562.

[36] C. Girardot, G. Lemercier, J.-C. Mulatier, J. Chauvin, P. L. Baldeck, C. Andraud, *Dalton Trans.* **2007**, 3421-3426.

[37] W. W. Weare, S. M. Reed, M. G. Warner, J. E. Hutchison *J. Am. Chem. Soc*., **2000**, *122*, 12890-12891.

[38] M. Montalti, A. Credi, L. Prodi, M.T. Gandolfi, Handbook of photochemistry, CRC Press, Boca Raton, **2006**.

[39] L. M. Lawson-Daku, J. Linares, M.-L. Boillot, *Phys. Chem. Chem. Phys.* **2010**, *12*, 6107-6123.

[40] J. Saltiel, B.W. Atwater, *Adv. Photochem*. **1988**, *14*, 1-85; M. Ciofalo, G. Ponterini, *J. Photochem. Photobiol. A: Chemistry* **1994**, *83*, 1-6.

[41] C. E. Powell, M. G. Humphrey, M. P. Cifuentes, J. P. Morrall, M. Samoc, B. Luther-Davies, *J. Phys. Chem. A*, **2003**, *107*, 11264-11266.

[42] A. de la Reberdière, F. Lachaud, F. Chuburu, C. Cadiou, G. Lemercier, *Tetrahedron Lett.,* **2012**, *53*, 6115-6118.

[43] S. R. Meech, D. Phillips, *J. Photochem.* **1983**, *23*, 193-217.

[44] S. D. Melgaard, D. V. Seletskly, A. Di Lieto, M. Tonelli, M. Sheik-Bahae, *Sensitive measurement of optical nonlinearities using a single beam*. IEEE Journal of Quantum Electronics, **1990**. 26(4): pp 760-769

[45] M. Samoc, A. Samoc, B. Luther-Davies, M. G. Humphrey, M.-S. Wong, Optical Materials, **2003**. 21(1-3): p. 485-488.

[46] M. Samoc, *et al.*, in *Multiphoton Processes in Organics and Their Application*, (Eds.: I. Rau and F. Kajzar), Old City Publishing, Philadelphia**, 2011**, pp. 341-355.

Received: ((will be filled in by the editorial staff))
Published online: ((will be filled in by the editorial staff))

Entry for the Table of Contents (Please choose one layout)

Layout 1:

ARTICLES

((Text for Table of Contents
375-475 characters, including spaces
Start with catchy bold text))

((Author(s), Corresponding Author(s)))*

Page No. – Page No.

((Title))

Layout 2:

ARTICLES

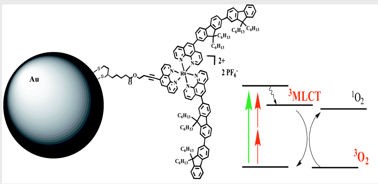

The synthesis and photophysical properties of gold nanoparticles functionalized with Ru(II) complexes (**AuNP-[Ru-PFF]**) are described. Z-Scan measurements reveal two-photon absorption (2PA) properties for both free Ru(II) complexes and related NPs; for higher energy (around 600 nm), 2PA properties are switched to saturable absorption for the NPs. Applications such as optical power limiting and oxygen sensitization can be anticipated.

Reference

J. Moreau[1] F. Lux, M. Four, J. Olesiak-Banska, K. Matczyszyn, P. Perriat, C. Frochot, P. Arnoux, O. Tillement, M. Samoc, G. Ponterini, S. Roux, G. Lemercier

Page No. – Page No.

A new 5-(difluorenyl)-1,10-phenanthroline-based Ru(II) complex as coating agent for potential multifunctional gold nanoparticles